colonizes and rapidly dies. The upper end of sapling mortality and growth distributions in America is set by gap specialists: *C. obtusifolia* at BCI (12% year^{-1} mortality, 14% year^{-1} growth), *C. sciadophylla* at Yasuni (5.0% year^{-1} mortality, 6.3% year^{-1} growth), and *C. monostachya* at La Planada (8.8% year^{-1} mortality, 8.2% year^{-1} growth). Diverse Southeast Asian forests lacked species with such high rates (*27*).

The most diverse tropical forests are the least diverse demographically. It remains plausible that demographic niches are packed more tightly in some forests than others, but this seems unlikely, because packing should depend only on population size and turnover, which do not vary much. Moreover, the successional-niche hypothesis is not favored by the strong peak in demographic rates near 1 to 2% year^{-1}; if demographic niches were crucial, then rates ought to be spread evenly over the entire range (*28*). Instead, the similarity in demography of many species suggests trait convergence (*29*). We believe that broad diversity differences are due to the source pool of different biogeographic regions, and that demographic differences play a minor role in species coexistence.

References and Notes

1. M. D. Swaine, D. Lieberman, F. E. Putz, *J. Trop. Ecol.* **3**, 359 (1987).
2. Most forest censuses cover a single hectare or less and include only larger trees. Except in Europe and North America, such small samples capture less than half the local species, with many represented by a single individual.
3. N. Pitman, J. Terborgh, M. R. Silman, P. Núñez V., *Ecology* **80**, 2651 (1999).
4. N. L. Stephenson, P. J. van Mantgem, *Ecol. Lett.* **8**, 524 (2005).
5. O. L. Phillips, P. Hall, A. H. Gentry, S. A. Sawyer, R. Vásquez, *Proc. Natl. Acad. Sci. U.S.A.* **91**, 2805 (1994).
6. D. Tilman, *Plant Strategies and the Dynamics and Structure of Plant Communities* (Princeton Univ. Press, Princeton, NJ, 1988).
7. S. W. Pacala, M. Rees, *Am. Nat.* **152**, 729 (1998).
8. B. M. Bolker, S. W. Pacala, C. Neuhauser, *Am. Nat.* **162**, 135 (2003).
9. M. Rees, R. Condit, M. Crawley, S. Pacala, D. Tilman, *Science* **293**, 650 (2001).
10. J. S. Clark, J. Mohan, M. Dietze, I. Ibañez, *Ecology* **84**, 17 (2003).
11. M. B. Bonsall, V. A. A. Jansen, M. P. Hassell, *Science* **306**, 111 (2004).
12. J. S. Clark, S. LaDeau, I. Ibañez, *Ecol. Monogr.* **74**, 415 (2004).
13. D. Tilman, *Proc. Natl. Acad. Sci. U.S.A.* **101**, 10854 (2004).
14. P. J. Grubb, *Biol. Rev. Camb. Philos. Soc.* **52**, 107 (1977).
15. S. J. Wright, *Oecologia* **130**, 1 (2002).
16. J. Silvertown, *Trends Ecol. Evol.* **19**, 605 (2004).
17. Table 1 includes 4956 species, but some occur at more than one site, and taxonomy has not been fully aligned across sites. We estimate 4500 different species at the 10 sites.
18. R. Condit, *Trends Ecol. Evol.* **10**, 18 (1995).
19. The Sarawak plot covers 52 ha. For comparison, the number 1167 was taken from a 50-ha subset.
20. J. K. Vanclay, *J. Trop. For. Sci.* **4**, 15 (1991).
21. R. Condit, S. P. Hubbell, R. B. Foster, *Ecol. Monogr.* **65**, 419 (1995).
22. A. Gelman, J. B. Carlin, H. S. Stern, D. B. Rubin, *Bayesian Data Analysis* (Chapman and Hall, Boca Raton, FL, 1995).
23. M. Liermann, R. Hilborn, *Can. J. Fish. Aquat. Sci.* **54**, 1976 (1997).
24. The rate constant m is the derivative of population size N with respect to time, $\frac{dN}{dt}$, due to mortality alone. It is approximated by $\frac{\ln N_2 - \ln N_1}{t_2 - t_1}$. Relative growth rate is $g = \frac{\ln dbh_2 - \ln dbh_1}{t_2 - t_1}$, where *dbh* is the stem diameter at breast height.
25. Materials and methods are available as supporting material on *Science* Online.
26. R. Sukumar, H. S. Suresh, H. S. Dattaraja, N. V. Joshi, in *Forest Biodiversity: Research and Modeling*, F. Dallamier, J. Comiskey, Eds. (Smithsonian, Washington, DC, 1998), pp. 495–506.
27. R. Condit *et al.*, *Phil. Trans. R. Soc. London Ser. B* **354**, 1739 (1999).
28. S. J. Wright, H. C. Muller-Landau, R. Condit, S. P. Hubbell, *Ecology* **84**, 3174 (2003).
29. S. P. Hubbell, *Ecology,* in press.
30. Errors in *dbh* measurements are 1 to 2 mm in saplings, and many saplings show slight negative growth (*25*). We, thus, cannot measure relative growth rates below about 0.5% year^{-1}. Where close to 0.5% year^{-1}, the low end of the sapling growth distributions are probably artifacts. In larger trees, errors are smaller relative to *dbh*, eliminating the problem.

31. Analyses were supported by NSF grant DEB-9806828 of the Research Coordination Network Program to the Center for Tropical Forest Science. Data collection was funded by many organizations, principally the NSF, Andrew W. Mellon Foundation, Peninsula Community Foundation, Smithsonian Tropical Research Institute, Arnold Arboretum (Harvard), Indian Institute of Science, Forest Research Institute of Malaysia, Royal Thai Forest Department, National Institute of Environmental Studies (Japan), and John D. and Catherine T. MacArthur Foundation. We thank the hundreds of field workers who have measured and mapped trees.

Supporting Online Material

www.sciencemag.org/cgi/content/full/1124712/DC1
Materials and Methods
Fig. S1
Tables S1 to S4
References
Database S1
Computer Codes

9 January 2006; accepted 31 May 2006
Published online 8 June 2006;
10.1126/science.1124712
Include this information when citing this paper.

A Single Amino Acid Mutation Contributes to Adaptive Beach Mouse Color Pattern

Hopi E. Hoekstra,[1]* Rachel J. Hirschmann,[1] Richard A. Bundey,[2] Paul A. Insel,[2] Janet P. Crossland[3]

Natural populations of beach mice exhibit a characteristic color pattern, relative to their mainland conspecifics, driven by natural selection for crypsis. We identified a derived, charge-changing amino acid mutation in the melanocortin-1 receptor (*Mc1r*) in beach mice, which decreases receptor function. In genetic crosses, allelic variation at *Mc1r* explains 9.8% to 36.4% of the variation in seven pigmentation traits determining color pattern. The derived *Mc1r* allele is present in Florida's Gulf Coast beach mice but not in Atlantic coast mice with similar light coloration, suggesting that different molecular mechanisms are responsible for convergent phenotypic evolution. Here, we link a single mutation in the coding region of a pigmentation gene to adaptive quantitative variation in the wild.

The identification of the specific molecular changes underlying adaptive variation in quantitative traits in wild populations is of prime interest (*1*, *2*). Pigmentation phenotypes are particularly amenable to genetic dissection because of their high heritability and our knowledge of the underlying developmental pathway (*3*). In a series of classic natural history studies (*4*, *5*), Sumner documented pigment variation in *Peromyscus polionotus*, including eight extremely light-colored "beach mouse" subspecies, which inhabit the primary dunes and barrier islands of Florida's Gulf and Atlantic coasts (*6*). This light color pattern is driven by selection for camouflage (*7*, *8*) as major predators of *P. polionotus* include visual hunters (*9*). Because the barrier islands on the Gulf Coast are <6000 years old (*10*), this adaptive color variation may have evolved rapidly.

We examined the contribution of the melanocortin-1 receptor gene (*Mc1r*) to this adaptive color patterning. MC1R, a G protein–coupled receptor, plays a key role in melanogenesis by switching between the production of dark eumelanin and light pheomelanin (*11*). Mutations in *Mc1r* have been statistically associated with Mendelian color polymorphisms in several mammalian species (e.g., *12–14*) and in natural variants of avian plumage (*15*, *16*).

[1]Division of Biological Sciences and [2]Department of Pharmacology, University of California, San Diego, La Jolla, CA 92093, USA. [3]*Peromyscus* Genetic Stock Center, Department of Biological Sciences, University of South Carolina, Columbia, SC 29208, USA.

*To whom correspondence should be addressed. E-mail: hoekstra@ucsd.edu

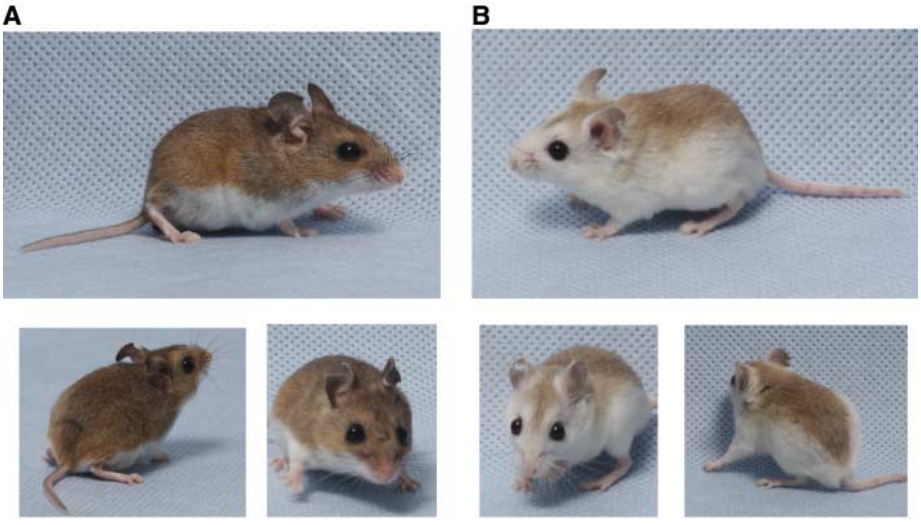

Fig. 1. Photographs of a typical (**A**) mainland mouse (*Peromyscus polionotus subgriseus*) and (**B**) Santa Rosa Island beach mouse (*P. p. leucocephalus*), highlighting the color pattern differences in the flank, face, and rump between these subspecies.

Table 1. Statistical association between allelic variation at *Mc1r* and seven pigmentation traits in 459 F_2 individuals. Phenotypes were categorically scored based on the pigmentation pattern on individual hairs in seven areas (traits). For all seven traits, each F_2 was scored as follows: 0, unpigmented hair; 1, partially pigmented hair; and 2, fully pigmented hair. The total number of F_2s with each phenotypic score is partitioned by *Mc1r* genotype for each trait: RR, homozygous for the dark *Mc1r* allele; RC, heterozygous; and CC, homozygous for the light *Mc1r* allele. The frequency of F_2s with each phenotype score is shown for each trait, with the phenotype of all F_1 individuals in bold. The mean phenotypic score (±SD) for each trait is provided and is also partitioned among each genotype. The percentage of variance explained by *Mc1r* genotype (PVE) and likelihood ratio chi-square (X^2) values are shown. *All seven tests were statistically significant ($P < 0.0001$).

Trait	*Mc1r* genotype	Phenotypic score			Mean ± SD	PVE (%)	X^2
		0	1	2			
Whisker		0.37	**0.30**	0.33	0.97 ± 0.84	11.5	115.3*
	RR	12	49	65	1.42		
	RC	69	77	69	1.00		
	CC	85	13	20	0.45		
Rostrum		0.11	0.18	**0.71**	1.61 ± 0.68	36.4	131.4*
	RR	0	0	126	2.00		
	RC	0	40	175	1.81		
	CC	49	42	27	0.81		
Cheek		0.14	**0.60**	0.26	1.12 ± 0.63	27.2	232.9*
	RR	0	91	35	1.28		
	RC	0	159	55	1.25		
	CC	66	23	29	0.69		
Eyebrow		0.16	0.25	**0.59**	1.42 ± 0.76	16.2	141.4*
	RR	0	21	105	1.83		
	RC	18	62	135	1.54		
	CC	56	31	31	0.79		
Ear		0.44	**0.36**	0.20	0.75 ± 0.77	10.2	98.0*
	RR	28	53	45	1.13		
	RC	89	79	47	0.80		
	CC	85	33	0	0.28		
Ventrum		**0.69**	0.11	0.20	0.51 ± 0.81	16.3	122.6*
	RR	55	27	44	0.91		
	RC	144	24	47	0.55		
	CC	118	0	0	0.00		
Ankle		0.45	**0.35**	0.20	0.75 ± 0.77	9.8	93.4*
	RR	24	70	32	1.06		
	RC	94	66	55	0.82		
	CC	88	26	4	0.29		

We sequenced the entire coding region of *Mc1r* [954 base pairs (bp)] in five Santa Rosa Island beach mice (*P. p. leucocephalus*) and five mainland mice (*P. p. subgriseus*) from colonies derived from wild populations (*17*). A single, fixed nucleotide polymorphism (SNP) occurs between the two subspecies, resulting in a charge-changing amino acid variant ($R^{65}C$) in the first intracellular loop of MC1R (fig. S1). To determine the ancestry of this mutation, we genotyped this SNP in 14 other *Peromyscus* species ($N = 45$ individuals) (table S1). These additional species are all fixed for R^{65} as in the mainland "dark allele," suggesting that the "light allele" is derived and not present in any other fully pigmented *Peromyscus* species.

To examine independently the relationship between this mutation ($R^{65}C$) and the derived light-colored phenotype, we generated a large reciprocal F_2 intercross between the Santa Rosa Island beach mouse and the mainland subspecies (Fig. 1). We characterized color phenotype for seven pigmentation traits, which provide an overall description of the continuous variation in color pattern, and genotyped the *Mc1r* allele in 459 F_2 individuals [126 with two dark *Mc1r* alleles (RR), 215 with one dark and one light allele (RC), and 118 with two light alleles (CC)]. Based on the observed phenotypic variation among F_2s, beach mouse color pattern has a multigenic architecture (Table 1). Pairwise correlation (R^2) between traits ranged from 0.147 to 0.500 ($P < 0.05$ for all comparisons), revealing a shared genetic basis among traits but also indicating the role of loci expressed in distinct spatial regions.

Two lines of evidence suggest that both dominant and recessive alleles contribute to the adaptive light color phenotype. First, all F_1 hybrids are intermediate in overall color pattern, with some traits resembling the mainland parent and other traits the beach mouse parent (Table 1). Second, dominance varies at the *Mc1r* locus itself. Phenotypic scores for pigmentation traits among F_2s are sometimes above the mean score of 1, suggesting that the light *Mc1r* allele is partially recessive, and sometimes below the mean score, suggesting that the light *Mc1r* allele is partially dominant (Table 1).

We found a significant statistical association between the $R^{65}C$ polymorphism and all seven traits, although the percentage of phenotypic variance explained by *Mc1r* varied (9.8% to 36.4%) (Table 1). For some pigmentation traits, the association between phenotype and *Mc1r* genotype was notable: All RR F_2s ($N = 126$) expressed the darkest phenotype on the rostrum and, conversely, only CC individuals expressed the lightest rostrum phenotype ($N = 49$). We calculated principal component scores for the combined color traits and evaluated whether there were

significant differences between the *Mc1r* alleles for PC1 scores (PC1 explained 71% of the variance in color traits); these analyses suggest that *Mc1r* accounts for 26% of PC1 ($P < 0.0001$). Together, these data indicate that *Mc1r* is a major effect locus on color pattern, having pleiotropic effects on pigmentation in spatially diverse areas of the body.

Functional tests of the light and dark *Mc1r* alleles demonstrate that the $R^{65}C$ amino acid mutation contributes to variation in adaptive pigmentation. We performed in vitro assays on HEK293T cells expressing light or dark *Peromyscus* coding region alleles at similar levels. Stimulation with an MC1R agonist (NDP-αMSH) and subsequent measurement of generated cyclic adenosine monophosphate (cAMP) by radioimmunoassay revealed that compared with dark receptor–expressing cells, cells that expressed the light MC1R had a statistically significant reduction in basal and stimulated cAMP formation (Fig. 2A) ($P < 0.05$, Student's t test, $n = 4$; maximum responses: dark allele = 120 ± 15 pmol/mg protein, light allele = 28 ± 5 pmol/mg protein). MC1R-mediated cAMP formation is associated with eumelanin production (*18*); thus, reduced cAMP production may underlie the lack of dark pigmentation observed in mice expressing the light MC1R.

The light MC1R displays lower affinity binding to αMSH, and the decreased response to guanine nucleotide by the light receptor implies an altered ability to interact with G proteins (Fig. 2B). Specifically, whereas the dark receptor displays a substantial GppNHp-promoted shift in IC_{50} (from 1.37 ± 0.01 nM in the absence to 13.5 ± 0.1 nM in the presence of GppNHp), the light allele has a decreased affinity for nucleotide and a nonsignificant IC_{50} shift (without GppNHp, 222 ± 30 nM; with, 178 ± 14 nM). These results demonstrate that a single amino acid mutation in MC1R is responsible for reduced ligand binding and G protein coupling, consistent with the reduced ability of the light MC1Rs to promote cAMP formation in vivo.

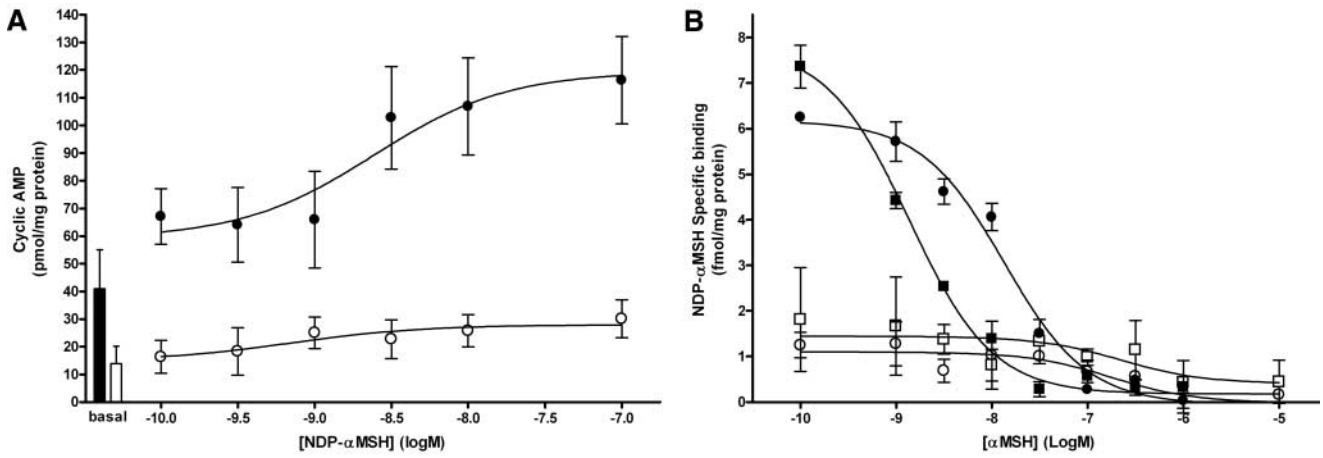

Fig. 2. Cyclic AMP and ligand-binding assays showing functional differences between light and dark *Mc1r* alleles. All data points are means ± SEM. (**A**) HEK293T cells transfected with dark MC1R (filled circles) or light MC1R (open circles) have different cAMP responses to NDP-αMSH stimulation. Bars indicate basal level of cAMP production in cells transfected with dark MC1R (black) and light MC1R (white); lines indicate standard error. (**B**) αMSH competition for $[^{125}I]$NDP-αMSH binding to HEK293T cells transfected with dark MC1R (filled symbols) or light MC1R (open symbols). Squares indicate assays without GppNHp and circles with GppNHp (100 μM).

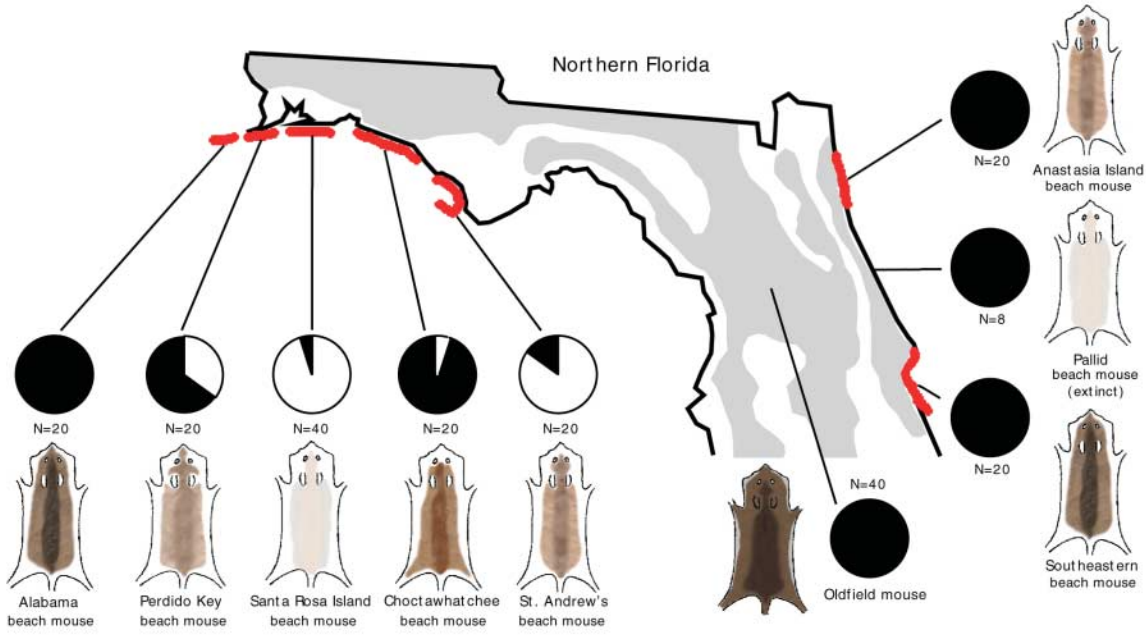

Fig. 3. Frequency of *Mc1r* alleles in one mainland and eight beach mouse subspecies from northern Florida. Images represent typical color patterns for each subspecies. Red areas represent the distribution of each beach mouse subspecies, and the gray area represents the range of mainland subspecies in Florida. Lines indicate sampling locales. Circles represent frequencies of the light *Mc1r* (white) and dark *Mc1r* (black) alleles identified. The number of alleles sampled is provided.

We next examined the frequency of *Mc1r* alleles in natural populations by genotyping the informative SNP in eight beach mouse subspecies and one mainland subspecies (Fig. 3 and table S2). In the Gulf Coast the light allele was at highest frequency (0.95) in the palest beach mouse subspecies, absent in the darkest subspecies, and at intermediate frequencies in the other subspecies (0.05 to 0.85) (Fig. 3). The distribution of *Mc1r* allele frequencies among Gulf Coast beach mice is not correlated with geographic distance. The light *Mc1r* allele was not detected in the mainland subspecies (0 of 40 alleles). In natural populations, different combinations of functionally distinct *Mc1r* alleles may contribute to variation in color patterning between mainland and Gulf Coast beach mouse subspecies, among the Gulf Coast subspecies, and within subspecies.

The derived *Mc1r* allele was absent from the similarly light-colored Atlantic coast beach mouse populations. We surveyed *Mc1r* allelic variation in two extant subspecies of beach mice and the extinct pallid beach mouse subspecies (~300 miles east of the nearest Gulf Coast beach mouse population) (Fig. 3). The absence of the derived *Mc1r* SNP from all three Atlantic coast subspecies suggests that the same mutation does not contribute to convergent phenotypic adaptation and that light coloration has evolved independently on the Atlantic coast.

This work has specific implications for understanding the evolutionary mechanisms responsible for adaptive phenotypic change. First, the identification and functional characterization of a single amino acid mutation's effect on quantitative variation provides a convincing exception to a growing number of examples demonstrating that variation in morphology is governed by changes in gene regulatory regions (*19*, *20*). Second, the observation that different combinations of alleles can produce similar pigmentation patterns suggests that distinct molecular mechanisms can underlie adaptive convergence even in similar selective environments (but see *21*). Finally, *Mc1r* represents a large effect locus, containing a quantitative trait nucleotide (QTN) contributing to variation in fitness, consistent with the view that adaptation may often proceed by large steps.

References and Notes

1. H. A. Orr, J. A. Coyne, *Am. Nat.* **140**, 725 (1992).
2. T. F. C. Mackay, *Annu. Rev. Gen.* **35**, 303 (2001).
3. I. J. Jackson, *Annu. Rev. Gen.* **28**, 189 (1994).
4. F. B. Sumner, *Proc. Natl. Acad. Sci. U.S.A.* **15**, 110 (1929).
5. F. B. Sumner, *Proc. Natl. Acad. Sci. U.S.A.* **15**, 481 (1929).
6. W. W. Bowen, W. D. Dawson, *J. Mamm.* **58**, 521 (1977).
7. M. C. Belk, M. H. Smith, *J. Mamm.* **77**, 882 (1996).
8. D. W. Kaufman, *J. Mamm.* **55**, 271 (1974).
9. J. L. VanZant, M. C. Wooten, *Biol. Conserv.* **112**, 405 (2003).
10. F. S. McNeil, *U.S. Geol. Surv.* **221**, 59 (1950).
11. G. S. Barsh, *Trends Gen.* **12**, 299 (1996).
12. E. Eizirik *et al.*, *Curr. Biol.* **13**, 448 (2003).
13. M. W. Nachman, H. E. Hoekstra, S. L. D'Agostino, *Proc. Natl. Acad. Sci. U.S.A.* **100**, 5268 (2003).
14. K. Ritland, C. Newton, H. D. Marshall, *Curr. Biol.* **11**, 1468 (2001).
15. N. I. Mundy *et al.*, *Science* **303**, 1870 (2004).
16. E. Theron, K. Hawkins, E. Bermingham, R. E. Ricklefs, N. I. Mundy, *Curr. Biol.* **11**, 550 (2001).
17. Materials and methods are available as supporting material on *Science* Online.
18. L. S. Robbins *et al.*, *Cell* **72**, 827 (1993).
19. S. B. Carroll, *PLoS Biol.* **3**, 1159 (2005).
20. S. B. Carroll, *Endless Forms Most Beautiful: The New Science of Evo-Devo* (Norton, New York, 2005).
21. P. F. Colosimo *et al.*, *Science* **307**, 1928 (2005).

22. We thank M. Dewey for help maintaining mice, and L. Mullen, L. Turner, and C. Yamada for contributions to the molecular work. Natural population samples were provided by M. Ashley, C. Parkinson, A. Suazo, and M. Wooten. Comments by the Hoekstra Lab, M. Hofreiter, J. Kohn, K. Peichel, T. Price, H. Roempler, J. Stinchcombe, and anonymous reviewers improved this manuscript. J.P.C. is supported by NIH-P40-RR14279 and NSF-DBI-0444165. This research is funded by NSF-DEB-0344710 to H.E.H. GenBank Accession Numbers: DQ482848, DQ482850.

Supporting Online Material

www.sciencemag.org/cgi/content/full/313/5783/101/DC1
Materials and Methods
Fig. S1
Tables S1 and S2
References

13 February 2006; accepted 27 April 2006
10.1126/science.1126121

Decay of Endoplasmic Reticulum-Localized mRNAs During the Unfolded Protein Response

Julie Hollien and Jonathan S. Weissman*

The unfolded protein response (UPR) allows the endoplasmic reticulum (ER) to recover from the accumulation of misfolded proteins, in part by increasing its folding capacity. Inositol-requiring enzyme–1 (IRE1) promotes this remodeling by detecting misfolded ER proteins and activating a transcription factor, X-box–binding protein 1, through endonucleolytic cleavage of its messenger RNA (mRNA). Here, we report that IRE1 independently mediates the rapid degradation of a specific subset of mRNAs, based both on their localization to the ER membrane and on the amino acid sequence they encode. This response is well suited to complement other UPR mechanisms because it could selectively halt production of proteins that challenge the ER and clear the translocation and folding machinery for the subsequent remodeling process.

The ER is responsible for the structural maturation of proteins entering the secretory pathway (*1*). When the folding burden on the ER exceeds its capacity, a collection of transcriptional and translational mechanisms termed the UPR is initiated (*2*). The UPR is essential for survival during ER stress and for development in metazoans (*3*, *4*), especially for the differentiation of secretory cells (*5*–*7*). A key sensor of the folding status of the ER is IRE1, a conserved transmembrane protein with an ER luminal sensor domain and cytosolic kinase and ribonuclease domains (*8*, *9*). Accumulation of misfolded proteins in the ER leads to the autophosphorylation and activation of IRE1, which cleaves specific sites in the mRNA encoding the transcription factor X-box–binding protein 1 (XBP-1) (*10*, *11*). This cleavage initiates an unconventional splicing reaction, leading to production of an active transcription factor. Although the sole output of IRE1 activation in yeast appears to be the splicing of the XBP-1 homolog HAC1 (*12*, *13*), several studies in metazoans suggest that IRE1 has additional functions not mediated by XBP-1 (*14*–*16*). Overexpression of IRE1 can also promote cleavage of the 28*S* ribosomal RNA (rRNA) (*17*) and the mRNA encoding IRE1 itself (*18*), which raises the possibility that, under some circumstances, the IRE1 nuclease can act on a broader range of substrates.

To systematically test the XBP-1 dependence of IRE1 outputs, we compared the changes in expression profiles associated with the UPR in *Drosophila* S2 cells depleted of either IRE1 or XBP-1 by RNA interference (RNAi) (Fig. 1, A and B). We induced the UPR with the reducing agent dithiothreitol (DTT), which prevents disulfide-linked folding, and analyzed the changes in expression of ~5000 genes using spotted DNA micro-

Department of Cellular and Molecular Pharmacology, University of California San Francisco, Howard Hughes Medical Institute, and the California Institute for Quantitative Biomedical Research, University of California San Francisco, San Francisco, CA 94143, USA.

*To whom correspondence should be addressed. E-mail: weissman@cmp.ucsf.edu